FTPC Calibration Run-VIII(dAu)-Procedure

October 2, 2009

1 Introduction

For each RHIC run period ambient conditions for the FTPC change and affect the true drift velocity. The relevant parameters are the gas temperature and the gas composition. The latter is determined by the setting of the flow meters, resulting in a stable composition throughout the running period (see Fig. 1). However, there remains an uncertainty in the absolute value of around 0.2 %. The temperature of the gas inside the sensitive volume of the FTPCs cannot be measured directly. There are calibrated temperature sensors on the aluminum body of the FTPCs. Their readings scatter over a range of about 2 degrees (see Fig. 2). We take the average of the measurements as the starting value of the calibration procedure and note that this average may not be the true temperature of the gas inside the FTPCs. Therefore a correction ('temperature offset') may be required. We have observed a small systematic drift of this average (< 0.3 degree) with time over the duration of the run period. Moreover, the FE cards are powered down during the filling of RHIC. The temperature in the off state is about 3 degrees lower and rises within about 40 minutes to the steady state value with the FEs on. In the following sections we describe the optimisation of the corrections to the temperature measurement and the gas composition for RHIC run VIII.

2 Gain Tables

The following pulser runs were used to obtain gain-tables:
8349044, 9013045, 9018068, 9021098, 9039141.

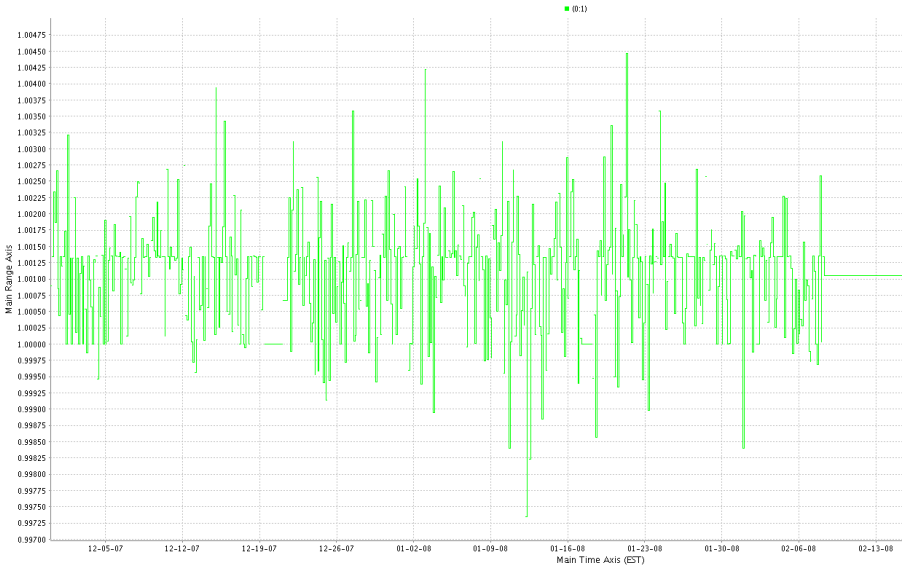

Figure 1: Slow control system measurements of the ratio of Ar to CO_2 flow versus time.

In addition physics runs throughout the run period were analysed to identify noisy or dead pads which were later excluded from the physics analysis by setting the corresponding gain factors to zero. The used runs were:
dAu: 8350051 (16/12/2007), 9013109, 9019008, 9022026 (22/1/2008)
pp: 9041043 (10/2/2008)

3 FTPC calibration with laser beams

Only laser run 8344094 (Dec.10, 2007, 16:16 EST, reversed full field), taken before the start of physics data taking, has all the RDO boards working and has sufficient track quality. All 3 beam parallel laser tracks were available in sector 2 which was then used for optimising the drift velocity by small adjustments of the temperature. First, the laser tracks were reconstructed with the set gas composition of $Ar/CO_2(50\%/50\%)$ and the average of the temperature measurements (24.05 (West) and 25.22 (East) degrees) and $t_0^{laser} = 1.57\mu$s. The position of the outer beam parallel laser beam is mainly determined by the value of t_0^{laser}. As shown by the two plots in the

top row of Fig. 3 and the comparison of surveyed and reconstructed positions in Table 1, the usyed value of 1.57 μs is correct.

	FTPCE			FTPCW		
	outer	middle	inner	outer	middle	inner
survey	28.41	19.44	11.85	28.51	19.45	11.68
reconstructed	28.44	19.40	11.85	28.49	19.48	11.68
deviation	00.03	00.04	00.00	-0.02	00.03	00.00

Table 1: Beam parallel laser beams in sector 2 (raft 8): surveyed and reconstructed radial positions in cm (extrapolated to the field cage end plane). Optimised temperature offsets of +1.35 and +3.80 degrees were used for FTPCE and FTPCW respectively (corresponding to temperature values of 26.47 and 27.76 degrees).

Since the inner laser beams did not reconstruct at the surveyed positions (radial position too large) temperature offsets of +1.35 and +3.80 degrees for FTPCE and FTPCW were introduced. With these offsets the reconstructed positions are moved to the correct positions as seen from Fig. 3 and Table 1. Note that the survey procedure (marking the laser beam positions on a sheet of paper and measuring the locations afterwards) probably has an accuracy of no better than 0.025 cm.

Next we tried to investigate whether the chosen combination of gas composition and temperature was resulting in an optimal drift velocity map. This can in principle be checked by studying the residuals of the inclined laser tracks. One should look for minima of

- width of the phi residual distribution (transverse projection should be a straight line for laser tracks, the mean residual is always close to zero due to the helix fit)
- 1/p from the helix fit (laser tracks are straight and should reconstruct as infinite momentum tracks)

by changing gas composition and temperature in such combinations which keep the reconstructed inner parallel laser beam at the surveyed radial position. A convenient procedure for carrying out such a scan does not exist yet. The available time did not allow us to complete the scan. Table 2 lists for the

ΔT		Δg	Difference(East)			Difference(West)		
East	West		Outer	Middle	Inner	Outer	Middle	Inner
-0.75	0.9	0.05	-0.04	0.04	-0.03	0.01	-0.05	-0.10
		0.12	-0.03	0.06	0.02	0.0	-0.02	-0.06
		0.15	-0.03	0.06	0.01	0.01	-0.02	-0.04
		0.18	-0.03	0.07	0.06	0.01	-0.01	-0.02
-1.0	1.0	0.05	-0.04	0.03	-0.06	0.01	-0.04	-0.09
		0.12	-0.04	0.05	0.01	0.01	-0.02	-0.04
		0.15	-0.03	0.05	0.01	0.01	-0.01	-0.02
		0.18	-0.03	0.06	0.03	0.01	-0.01	0.0
1.0	1.2	0.05	-0.03	0.12	0.17	0.01	-0.03	-0.06
		0.12	-0.02	0.14	0.23	0.01	-0.01	-0.02
		0.15	-0.02	0.15	0.24	0.01	0.0	0.0
		0.18	-0.02	0.15	0.26	0.01	0.0	0.02

Table 2: Deviations of reconstructed beam parallel lasers from measured positions for different temperature and gas offsets.

analysed combinations of changes (Δg change in % from 50/50 composition, ΔT change in degrees from optimised temperature offset) the deviations of the reconstructed parallel laser beams from the surveyed positions. It can be seen that only a few combinations are useful for the study. The range of the changes is not sufficient and the results are inconclusive.

Figure 4 shows for the optimised temperature offstes and the 50/50 gas composition the distribution of the residuals in the azimuthal (phi) direction and of the values of 1/p obtained from helix fits. The latter should ideally be zero. The fact that they are finite demonstrates that there remain some systematic distortions. One should in future also take laser runs with magnet off in order to find out whether these remaining distortions are due to imperfect correction of the ExB effect or are caused by other problems.

4 Determination of FTPC rotation corrections and check of t_0 from d+Au data

Dismounting and remounting of the FTPCs can lead to slight angular misalignments with respect to the TPC. Since we use the event vertex point

reconstructed by the TPC to improve the fitted momentum accuracy, we determine small corrections for each run period (after the TPC corrections have been finalised). We used the low-intensity, 6 on 6 bunches, runs 8348078 - 8348091 for this purpose. Reconstruction employing the temperature offsets optimised with the laser beams and the value of $t_0^{data} = 2.70\mu$s surprisingly showed a deviation of the radial step of the reconstucted cluster positions from the inner cathode position of 7.8 cm in FTPCW. In fact, the drift velocity seemed too large and indicated that the temperature offset needs to be reduced from 3.8 to 2.8 degrees. With this change the radial steps come out at the right positions as demonstrated by Fig. 5. We do not have an explanation for this inconsistency.

We can next proceed to the determination of the rotation corrections. Figure 6 shows distributions of the differences between the x,y positions of the event vertices determined from the FTPCs and the main TPC.

Small shifts are clearly seen in Fig. 6 and their values are listed in Table 3. From these the reconstruction program derives the necessary rotation corrections taking into account the location of the mounting points of the FTPC. The difference plots shown in Fig. 7, obtained after applying these small rotations during the reconstruction, demonstrate the success of the correction.

	FTPCE	FTPCW
observedVertexOffsetX	-0.05567	-0.12830
observedVertexOffsetY	0.10610	-0.14330

Table 3: Database entries of differences (cm) between vertex positions reconstructed in the FTPCs and the TPC using temperature offsets of 1.35 and 2.80 degrees in FTPCE and FTPCW respectively and $t_0^{data} = 2.70\mu$s (by convention the signs are reversed for X compared to the values derived from the plots in Fig. 6).

A further consistency check of the drift velocity calibration and the emloyed value of t_0^{data} is provided by a comparison of the z (longitudial) positions of the event vertices obtained from the FTPC and the TPC. The distributions of these differences are plotted in Fig. 8. The systematic shifts are small and of opposite sign for West and East. To compensate we decided to increase t_0^{data} slightly to 2.73 μs.

Run	Type	Radial step	
		FTPCE	FTPCW
8348091	dAu (low intensity)	7.85	7.76
9008010	dAu	7.82	7.73
9027041	dAu	7.88	7.70
9059022	pp	7.81	7.78

Table 4: Stability of radial steps through-out the run. Temperature offsets 1.35 and 2.80 degrees in FTPCE and FTPCW; $t_0^{data} = 2.70$ μsec.

5 Stability of the radial steps in physics runs

To study the stability of the calibration through the run period we checked the radial steps using the temperature offsets, gas compositions and t_0 obtained from the described calibration procedure. The runs used for this study and the obtained radial step values are listed in Table 4 and the corresponding plots are shown in Fig. 9. We find that the stability is satisfactory. However, we noticed that the radial step is steeper in FTPCE than in FTPCW. We have no explanation for this feature.

6 Epilogue

Unfortunately the value of t_0^{data} which got into the database for run 8 in May 2008 was 2.59 insted of 2.73 μsec. The subsequent production was done with this incoorect value resulting in a radial step at a position (see Fig. 10) which is too high by about 2 mm (averaged over both FTPCs). For any physics analysis this error is probably not very serious, but one should nevertheless be aware of it. The correct value was now (29/7/2009) put into the database retroactively, but the production has not been rerun.

7 Acknowledgement

The results discussed in this writeup were obtained by the combined efforts of A. Lebedev, N.K. Pruthi, J. Seyboth, P. Seyboth and M. Skoby.

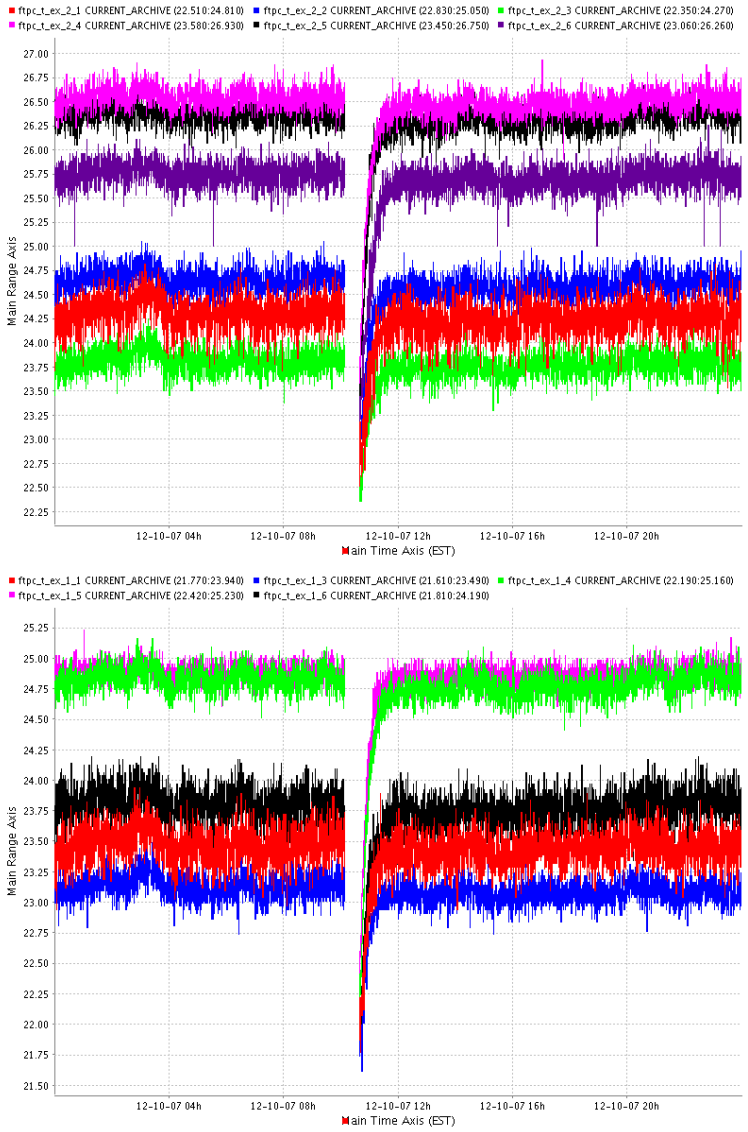

Figure 2: Slow control system measurements of the "extra" temperatures versus time around the laser run 83440094 on 10/12/2007 at 16:16 EST. Top (bottom) panel shows FTPCE (FTPCW). The plots clearly show the transient when switching on the FEs.

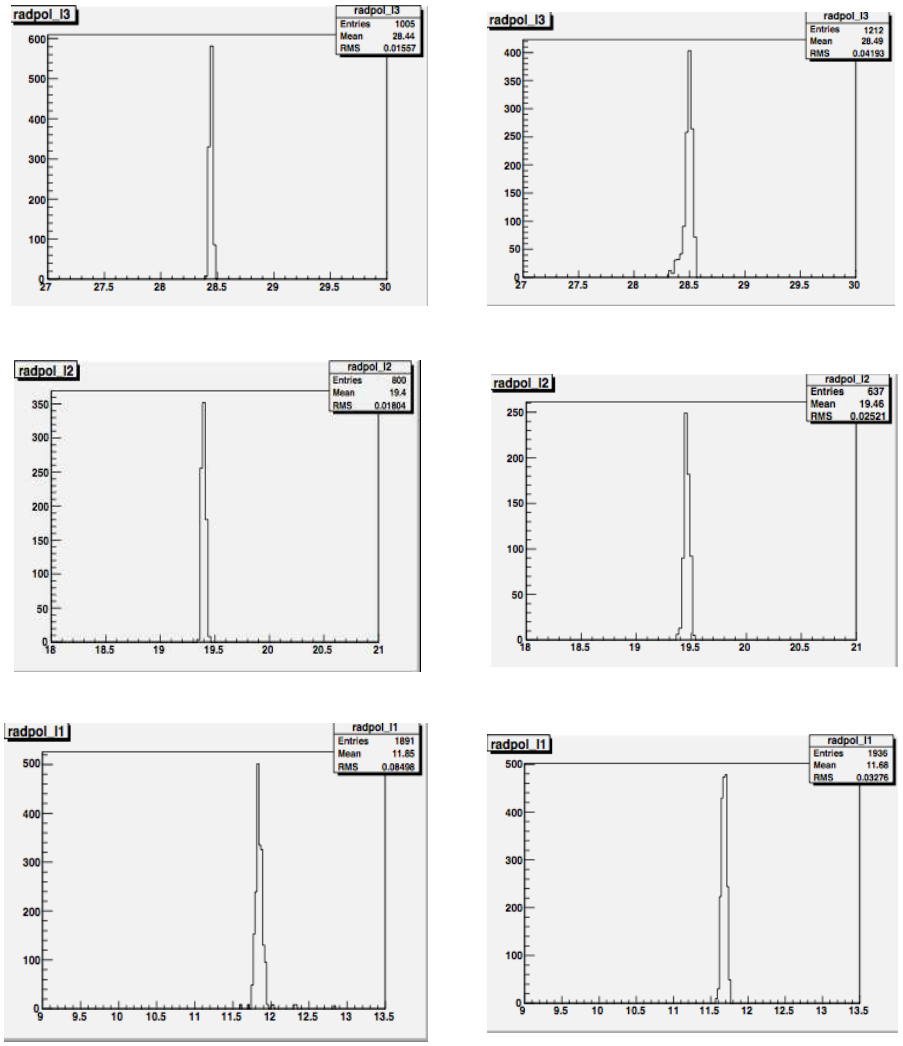

Figure 3: Reconstructed positions of beam parallel laser tracks in sector 2 (extrapolated to the outer field cage surface) for gas composition of $Ar/CO_2(50\%/50\%)$, $t_0^{laser} = 1.57\mu$s, $T_{East} = 26.47$ and $T_{West} = 27.76$ degrees. Left(right) column shows FTPCE(FTPCW), top, middle and bottom row show outer, middle and inner beams, respectively.

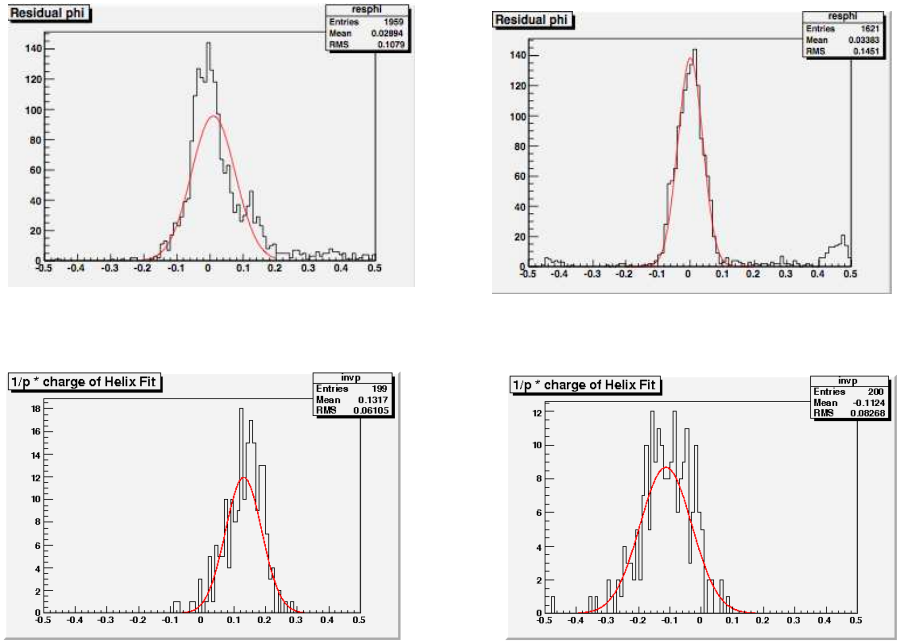

Figure 4: Inclined laser beams in FTPCE (laser beam 1, left column) and FTPCW (laser beam 5, right column) reconstructed with $T_{East} = 26.47$ and $T_{West} = 27.76$ degrees and gas composition of $Ar/CO_2(50\%/50\%)$. Plots show the distributions of azimuthal residuals (top row) and of 1/p obtained from helix fits (bottom row).

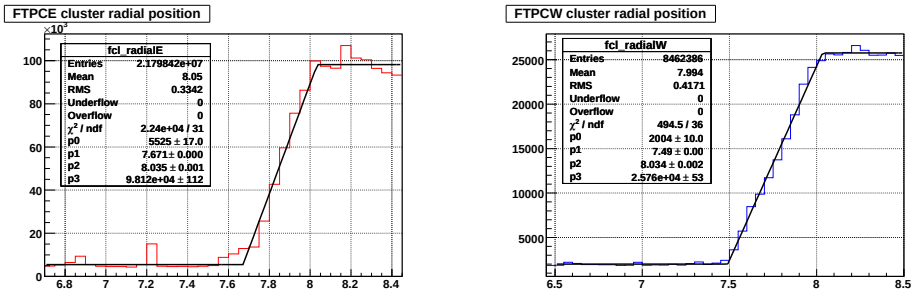

Figure 5: Reconstructed cluster positions in FTPCE (left) and FTPCW (right) for low-intensity run 8348091 showing the radial step with fitted lines. Temperature offsets were 1.35 and 2.80 degrees for FTPCE and FTPCW respectively and $t_0^{data} = 2.70\mu$s.

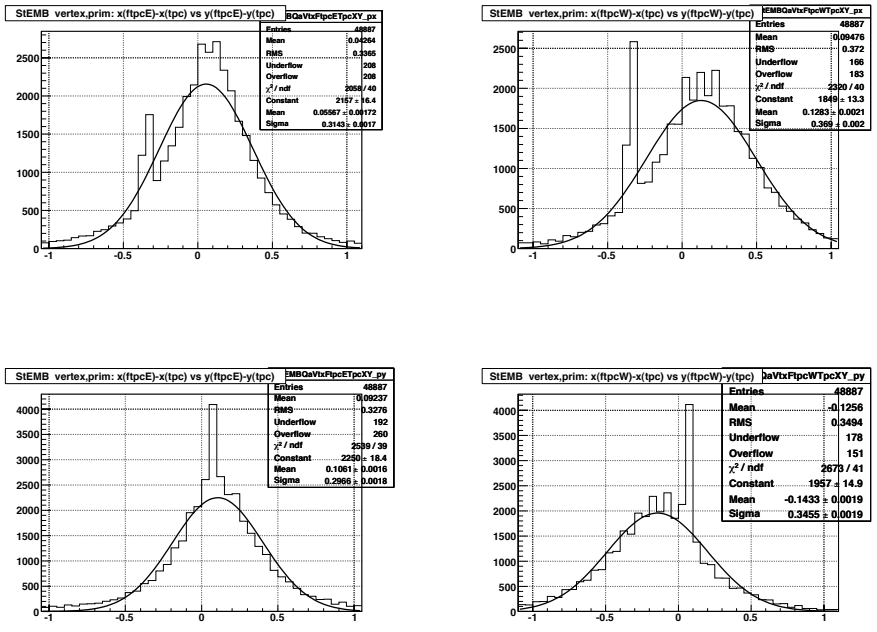

Figure 6: Differences between the x,y positions of the event vertices determined from the FTPCs and the main TPC. Left column: FTPCE, right column FTPCW; top row X_V^{FTPC} - X_V^{TPC}, bottom row Y_V^{FTPC} - Y_V^{TPC}.

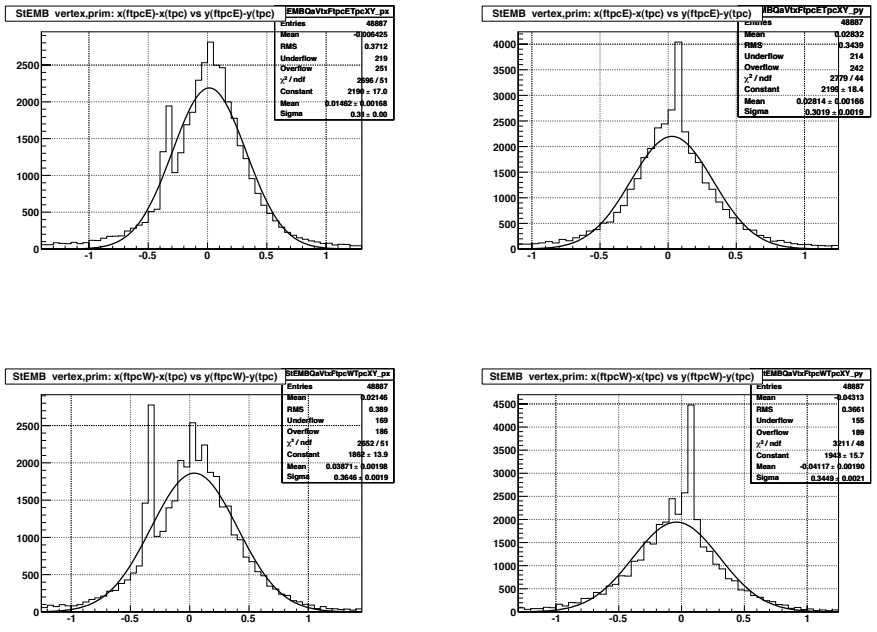

Figure 7: Differences between the x,y positions of the event vertices determined from the FTPCs and the main TPC after applying rotation corrections. Left column: FTPCE, right column FTPCW; top row X_V^{FTPC} - X_V^{TPC}, bottom row Y_V^{FTPC} - Y_V^{TPC}.

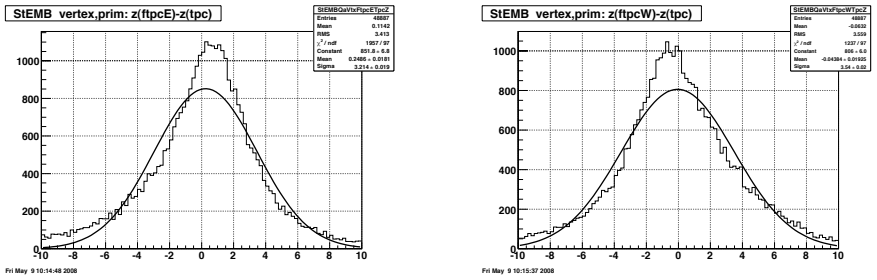

Figure 8: Differences Z_V^{FTPC} - Z_V^{TPC} between the z positions of the event vertices determined from the FTPCs and the main TPC after applying rotation corrections. Left: FTPCE, right FTPCW.

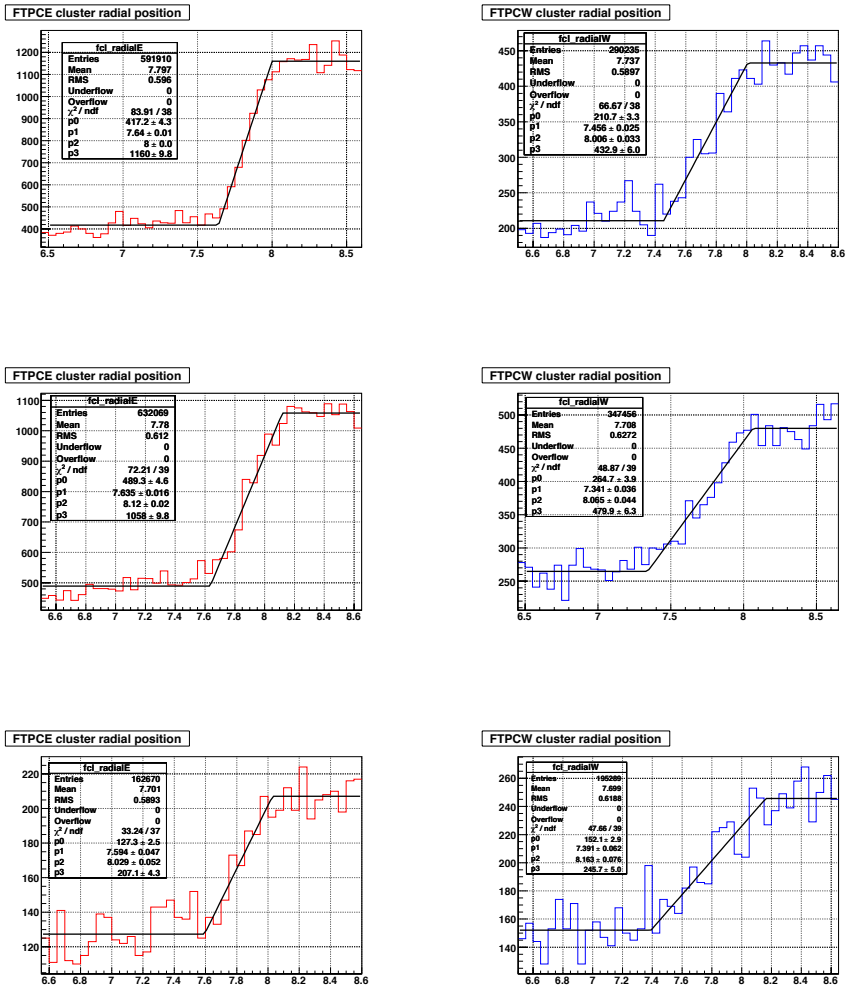

Figure 9: Stability study of radial steps through run VIII: FTPCE on left, FTPCW on right. Results are shown (from top to bottom) for d+Au runs 9008010, 9027041 and p+p run 9059022.

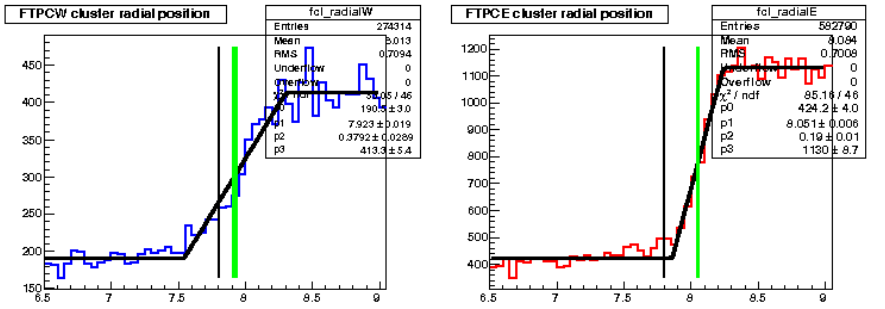

Figure 10: Radial steps in production d+Au run 9019023 ($t_0^{data} = 2.59$ μsec).